Fuel 254 (2019) 115582

Contents lists available at ScienceDirect

Fuel

journal homepage: www.elsevier.com/locate/fuel

Full Length Article

Sulfur free supported MoCx and MoNx catalysts for the hydrotreatment of atmospheric gasoil and its blends with rapeseed oil

Héctor De Paz Carmona*, Jan Horáček, Zdeněk Tišler, Uliana Akhmetzyanova

Unipetrol Centre for Research and Education, Block 2838, 436 70 Litvínov-Záluží 1, Czech Republic

ARTICLE INFO

Keywords:
Molybdenum nitride
Molybdenum carbide
Hydrotreatment
Sulfur
Vegetable oil
Co-processing

ABSTRACT

Generally, the commercial catalysts for hydrotreatment in refineries are supported sulfide transition-metal-based catalysts. However, the co-processing of vegetable oils reduces their hydrodesulfurization (HDS) efficiency by leaching sulfur from the active sites of the catalyst. The present work reports the use of six sulfur-free MoCx and MoNx catalysts (supporter with Al_2O_3, TiO_2 or ZrO_2) for the hydrotreatment of atmospheric gasoil (AGO) and co-processing of rapeseed oil (RSO – 5, 10 and 25 wt%). The screening tests were carried out in a fixed bed reactor at industrial operating conditions (330–350 °C, 5.5 MPa, WHSV = 1–2 h^{-1}). Higher reaction temperatures and lower WHSV had a positive effect on catalyst activity and product quality. In case of co-processing, the hydrodeoxygenation reaction mechanism was found to be dominant, producing n-C_{16} and n-C_{18} n-alkanes at all AGO/RSO ratios used. Overall, our results suggest that alumina supported catalysts are the most promising materials, exhibiting a combination of excellent stability, high activity and no negative effects on HDS efficiency during AGO/RSO co-processing.

1. Introduction

Based on the need to reduce the greenhouse gas emissions due to automotive transportation and improve the security of fuel supplies, the European Council agreed in 2014, the 2030 framework for climate and energy. This framework sets out the European Union (EU) target of 27% as the share of renewable energy consumed in the EU in 2030. These energy agreements reveal the commitment and the ambitious strategy of the EU for renewable energy. Related to this strategy, the directives 2009/28/EC and 2009/30/EC support and promote the development of new, more efficient and environment-friendly biofuel technologies.

Advanced biofuels, produced from lignocellulosic (forestry and agricultural residues, energy crops, etc.) or triglyceride feedstock (vegetable oils, animal fats, etc.), can satisfy the energy requirements of the EU, as stipulated for the field of biofuels. In this sense, the lignocellulosic feedstocks are easier to transform into biofuels by gasification, fast pyrolysis or hydrolysis for the production of sugar monomers. During the gasification process, many complex reactions occur, including pyrolysis, partial oxidation and steam reforming. Syn-gas, composed mainly of CO_2, CO, CH_4, H_2 and N_2, is a typical product of lignocellulose gasification. A set of reactions take place during biomass fast/flash pyrolysis (hydrolysis, dehydration, isomerization, dehydrogenation, aromatization, etc.), which result in the formation of a dark brown liquid called bio-oil. However, this biofuel typically has a high viscosity, low heating value and is usually chemically unstable. The use of bio-oil in internal combustion engines requires complex upgrading [1]. Therefore, industrial implementation of these biofuel production processes is technologically difficult, because low-cost and effective processing technologies have not yet developed sufficiently.

On the other hand, triglyceride-based feedstock is usually more expensive than lignocellulosic feedstock, but can be more easily and efficiently converted into automotive fuels. The easiest and most common way to produce biofuels from triglycerides is transesterification into fatty acid methyl esters, well known as FAME [2]. However, catalytic hydrotreatment of triglycerides at high temperatures and pressures (300–400 °C and 50–70 bar) for deoxygenation has become a very interesting route to biofuels owing to the production of oxygen-free and stable hydrocarbons with attractive properties for diesel oil blending. This process has already found realtime application in petroleum industry in the form of co-hydroprocessing with atmospheric gas oils (AGOs) in hydrodesulfurization (HDS) units [3].

This catalytic co-processing involves the removal of sulfur, nitrogen, and metals from the petroleum feedstock, as well as the removal of oxygen from triglycerides and free fatty acids. The deoxygenation reaction includes three parallel steps: (i) hydrodeoxygenation (HDO) and (ii) (hydro)decarboxylation/(iii) (hydro)decarbonylation (HDC) [4].

* Corresponding author.
E-mail addresses: hector.carmona@unicre.cz (H. De Paz Carmona), horacekj.unicre@seznam.cz (J. Horáček), zdenek.tisler@unicre.cz (Z. Tišler), uliana.akhmetzyanova@unicre.cz (U. Akhmetzyanova).

https://doi.org/10.1016/j.fuel.2019.05.165
Received 17 November 2018; Received in revised form 31 January 2019; Accepted 30 May 2019

During co-hydroprocessing with fossil streams, triglycerides are transformed into hydrotreated vegetable oil (HVO), which is also known as green diesel. HVO consists mostly of linear paraffins with an even (16–18) or odd (15–17) number of carbon atoms. The distribution of "even" and "odd" paraffins depends on the selectivity to the HDO and HDC reaction mechanisms, which is determined by the combination of catalyst type and operating conditions [5]. Liquid water and light gases (propane, methane, CO_x) are the side products of the triglyceride deoxygenation. CO_x, as a reaction intermediate, can interact with the active sites and affect the catalytic activity [6]. These gaseous side products can also increase the amount of hydrogen consumed by the side reactions such as methanation of CO_x or reverse water gas shift reaction.

At present, the most common commercial catalysts for hydrotreatment in refineries are supported sulfide transition-metal-based catalysts. These catalysts utilize molybdenum and tungsten as the active metals, while nickel and cobalt are used as promoters. The typical catalyst supports are alumina (Al_2O_3) and silica (SiO_2) and their respective derivatives. Many reports on the hydroprocessing of vegetable oils (pure and waste) [7,8] and their co-hydroprocessing with petroleum feedstocks (heavy vacuum gas-oil, AGO, etc.) [9,10] have been published. These studies showed the viability of this co-processing on the industrial scale involving hydrotreatment units in a petroleum refinery.

One of the most important parameters of co-processing is the reduction of HDS efficiency due to the competitive reactions of triglyceride deoxygenation. Another aspect reducing the HDS efficiency is the leaching of sulfur from the active sites of the catalyst during the hydrotreatment of triglycerides [11]. Additional problems related to a significantly higher heat of reaction compared to the conventional HDS processes result in the possibility of the reactor overheating. These problems are solved by co-processing triglycerides with fossils instead of treating pure triglycerides. The optimal triglyceride content in the feed unit is 5–10 wt% [12].

In this manner, the use of a sulfur-free catalyst such as molybdenum carbide or nitrides presents a promising approach to resolving the problems associated with sulfur loss from the active sites. Some previous studies on these catalysts focused on their suitability for the hydrogenation of various chemical compounds [13], which is based on their capacity to adsorb/activate hydrogen and transfer it to the reactant molecules, which is a mandatory requirement for exhibiting hydrogenation activity.

Superior activity of the catalysts, especially towards hydrodenitrification (HDN), was observed in some comparative hydrotreatment studies of model compounds (benzothiophene and thiophene) [14,15] that used sulfide catalysts and mono- and bimetallic supported carbides and nitrides in batch and atmospheric flow reactors. Likewise, the studies of Da Costa et al. [16,17] on 4,6-dimethyldibenzothiophene and low-sulfur gas oils showed that for deep hydrotreated gas oils (< 50 wt. ppm of sulfur), the phosphorus-promoted molybdenum carbide catalysts were more active than the corresponding commercial catalyst in the HDS and HDN reactions.

Triglyceride hydrotreatment over supported carbides and nitrides has been well investigated. Several experiments using supported molybdenum carbide and nitride catalysts have been carried out. The results showed high vegetable oil conversions of around 98–100% [18] in a continuous micro-reactor over β-Mo_2C catalyst. The effect of the support during soybean oil hydrotreatment over NiMo carbide catalysts was also studied; the results showed a high production of green diesel, consisting of C_{15}–C_{18} hydrocarbons, over meso-porous γ-Al_2O_3 and Al-SBA-15 supported catalysts [19].

Industrially, the highest amount of material subjected to hydrotreatment involves the petrochemical processes for fuels and the production of petrochemicals. Refinery processes require typically very large amounts of catalysts in the reactors than is usually employed in fine chemical and pharmaceutical applications. A long lifetime, adequate activity, price and sulfur (sulfane) resistance are the key requirements of a catalyst employed in refineries.

This paper describes an extensive and detailed study of six sulfur-free molybdenum carbide (MoCx) and nitride (MoNx) supported (Al_2O_3, TiO_2 and ZrO_2) catalysts during the hydrotreatment of AGO and its blends with rapeseed oil (RSO − 5, 10 and 25 wt%) at industrial operating conditions (330–350 °C and 5.5 MPa). The aim of this work was to study the catalysts properties (fresh and used), as well as the effect of the operating conditions (temperature and space velocity) and triglycerides co-processing on the product quality and catalyst activity (defined as the HDS, HDN and hydrogenation), in order to be able to compare them with conventional sulfide catalysts.

2. Experimental

2.1. Catalyst synthesis

Six molybdenum catalysts were synthesized by incipient wetness impregnation of the catalytic supports Al_2O_3, TiO_2 and ZrO_2. Each support was loaded with the molybdenum precursor. The materials were then thermally treated to prepare molybdenum carbide and nitride for a comparison of the active phases in AGO hydrotreatment and triglyceride co-processing, respectively.

Hexamethylenetetramine molybdenum complex, which was synthesized according to Afanasiev method [20], was used as the molybdenum precursor. The precursor was loaded into the support particles (Al_2O_3, TiO_2 or ZrO_2) with sizes of 224–560 μm. Then, the catalyst was dried at 120 °C for 12 h. The formation of the carbide or nitride active phase was achieved by temperature-programmed reduction in a tubular quartz reactor with overall length of 140 cm and heated zone length of 100 cm. The reactor tube was placed inside a triple-zone electric heater that was controlled by PID regulators. The support impregnated with the precursor was placed into a cuvette, then, thermal treatment commenced under the flow of 20 vol% CH_4 in H_2 or 20 vol% H_2 in N_2, depending on whether the active phase was carbide or nitride. The thermal treatment involved starting at 200 °C and reaching 700 °C at the rate of 10 °C/min. The catalyst was held at the final temperature for 3 h. Then, the reactor was cooled under the gas flow to ambient temperature. Finally, the catalyst was passivated with 1 vol% O_2 in argon. The freshly prepared catalysts were then characterised by X-ray diffraction (XRD; Philips APD 1700), inductively coupled plasma (ICP; Agilent 725), nitrogen physisorption (BET – Chemisorption Analyzer Micromeritics AutoChem 2950 HP) and elemental analysis (FLASH 2000 Combustion CHNS/O Analyzer).

2.2. Catalytic tests

Screening experiments were carried out in a stainless steel continuous fixed bed reactor with the internal diameter of 17 mm, with a thermowell with the outer diameter of 5 mm placed in the axis of the reactor. The reactor was equipped with a triple-zone electric heater that had independent controls for each zone. The experimental unit was equipped with high- and low-pressure product collectors, and the pressure in the system was controlled by a Kämmer regulation valve that was placed behind the product collectors. The unit was placed in the experimental facility of UniCRE (Unipetrol Centre of Research and Education) in Litvínov-Záluží, Czech Republic. Fig. 1 shows a simplified scheme of the reactor used.

Prior to each test, the catalyst bed, with the particle size range 224–560 μm, was divided into four parts and diluted with fine inert SiC (10 μm) in the ratios 1:1, 1:2, 1:3 and 1:4 (vol:vol). The catalyst-SiC mixtures were then loaded into the reactor, from 1:1 to 1:4. This resulted in a gradual increase in the catalyst concentration along the catalyst layer in the direction of flow of the reactants. This loading procedure helps to maintain the reaction temperature profile in the isothermal regime. After the catalyst loading, the reactor was flushed

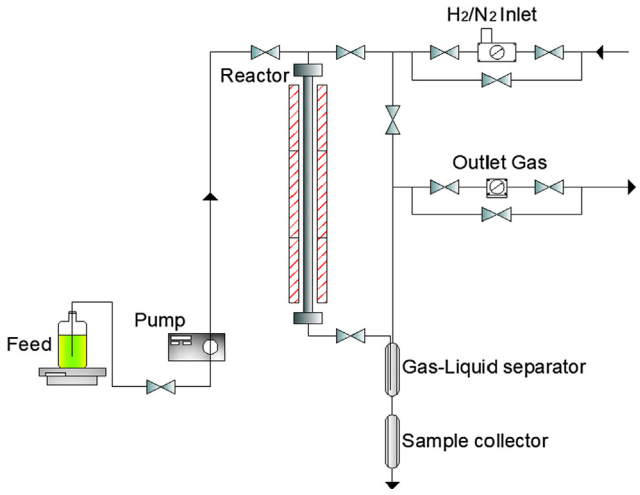

Fig. 1. Simplified scheme of the experimental reactor.

with N_2 (600 NL/h) at ambient temperature and atmospheric pressure for 2 h. Then, the gas was changed from N_2 to H_2 and the reactor was pressurized to 5.5 MPa under H_2 flow of 50 NL/h. Subsequently, the catalyst was treated under H_2 flow at 450 °C (heating rate 20 °C/h). Finally, the temperature was reduced to 330 °C and the H_2 flow adjusted to correspond to g/L = 1 NL/g/h.

The experiments were performed in the reaction temperature range 330–350 °C at the pressure of 5.5 MPa. The AGO obtained from industrial atmospheric distillation of Russian export blend crude oil was used as the main feedstock. AGO mixtures with 5, 10 and 25 wt% RSO (food quality) were used as the model feedstocks for co-processing hydrotreatment. Table 1 shows the basic properties of the AGO and RSO feedstocks.

Each catalyst was tested by screening with nine sets of experimental conditions. The effects of reaction temperature, RSO content in the feed and weight hourly space velocity (WHSV [g_{feed}/g_{cat}/h]) on product quality were investigated in each test. The same methodology of testing was used for all the catalysts to allow the comparisons of the active phases and of the effects of catalyst supports under different reaction conditions. The timeline of the screening experiment is shown in Table 2.

In the same way, Fig. 2 shows the variations in the density and refractive index at 20 °C during the entire experiment with MoCx/Al_2O_3 catalyst. The changes can be attributed to the different conditions used during the testing.

The liquid products were sampled from the low-pressure collector and weighed. For all the products, the density (ASTM D 4052) and refractive index (ASTM D 1218) at 20 °C were determined through routine measurements. More detailed characterisation was performed for the samples collected at steady state, which was determined by constant density and refractive index values. Sulfur (ASTM D 1552) and nitrogen (ASTM D 5291) contents, elemental analysis (ISO 29541), bromine number (ASTM D 1492) and acidic number (ASTM D 664) were determined for the steady-state samples. The boiling point distribution was determined as well by simulated distillation (Simdis) analysis, according to ASTM D 2887 method. The off-gas quality was characterized by gas chromatography (GC) with FID and TCD detectors (RGA: refinery gas analysis). Gas samples were collected only at the end of each period at steady state, before the reaction parameters changed.

After the experiment was complete, the spent catalyst was collected and separated from the inert SiC by using a sieve and washed in toluene by using soxhlet extractor. The washed catalyst was analysed using the same analytical techniques as those employed for the fresh catalyst (XRD, ICP, BET and elemental analysis).

The initial period of the experiment was used as the reference state for a comparison of the products obtained from the other sections. Sections 4 and 8 were added to determine the effects, if any, of the reaction temperature change and the co-processing reaction, respectively, on the catalytic activity. The effects of the changes in the reaction conditions were compared with the reference data obtained from the initial part of the experiment.

Table 1
Basic feedstock properties.

Property	Atmospheric gas oil	Rapeseed oil
Density at 20 °C, kg/m^3	852.6	914.5
Refractive index at 20 °C	1.4759	1.4725
Sulfur content, wt ppm	11010.0	2.2
Nitrogen content, wt ppm	239	1.3
Acid number, mg KOH/g	0.04	0.18
Bromine index, mg Br/g	8534	19,000
Carbon content, wt%	86.0	77.3
Hydrogen content, wt%	13.3	11.8
Oxygen content*, wt%	–	10.9

* Calculated by subtracting the carbon and hydrogen contents from 100.

Table 2
Chronological description of the reaction conditions of the screening experiment.

No.	TOS, h	T, °C	P, MPa	WHSV, h^{-1}	Feed*
1	0–40	330	5.5	2	AGO
2	40–64	340	5.5	2	AGO
3	64–88	350	5.5	2	AGO
4	88–112	330	5.5	2	AGO
5	112–136	330	5.5	2	AGOR_5
6	136–160	330	5.5	2	AGOR_10
7	160–184	330	5.5	2	AGOR_25
8	184–208	330	5.5	2	AGO
9	208–256	330	5.5	1	AGO

* AGOR_X: mixtures of AGO and RSO, X = content of RSO (wt%).

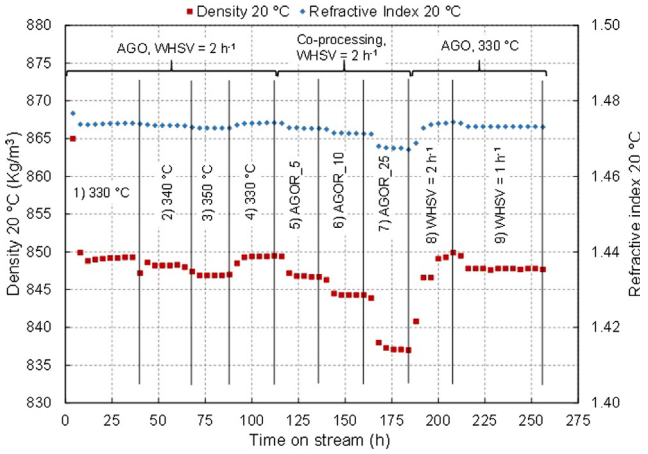

Fig. 2. Variations in the density and refractive index at 20 °C during the testing of MoCx/Al_2O_3.

2.3. Catalytic activity

The catalytic activity was determined based on the HDS and HDN efficiencies. These parameters were calculated as the percentages of sulfur and nitrogen removed from the AGO compounds. The HDS efficiency was determined according to the following equation:

$$HDS(\%) = \frac{(S_0 - (S_p \cdot \eta))}{S_0} \cdot 100 \quad (1)$$

where S_0 and S_p represent the sulfur contents of the feedstock and the

liquid product, respectively (wt. ppm). Similarly, 'η' represents the process yield, which is defined as the mass ratio between the desulfurized gasoil obtained and the liquid feedstock. Analogously, the HDN efficiency can be determined by using the nitrogen content, through the following equation:

$$HDN(\%) = \frac{(N_0 - (N_p \cdot \eta))}{N_0} \cdot 100 \quad (2)$$

where N_0 and N_p represent the nitrogen contents of the feedstock and the liquid product, respectively. These parameters have been determined for each relevant step of the experiments to evaluate the catalytic activity and how it changes with the operating conditions or the addition of RSO.

3. Results and discussion

Sulfur-free supported catalysts (MoCx and MoNx) were studied as alternatives to the conventional sulfide catalysts by investigating the effects of operating conditions and the addition of vegetable oil on product properties and catalyst suitability.

3.1. Catalyst characterization

The impregnation of the catalyst supports resulted in differences between these materials. The highest amount of molybdenum was loaded into the Al_2O_3 support (20–21 wt%), while the molybdenum contents of the ZrO_2 catalysts were only between 7.8 and 8.2 wt% (Table 3).

These results are in good agreement with the determined specific surface area, which revealed the highest value for the Al_2O_3-supported catalysts and nearly identical values for the TiO_2 and ZrO_2 catalyst supports. The higher amounts of molybdenum loading into the TiO_2-based catalysts were reflected in the different porous properties of both materials. Carburization was more effective in the case of TiO_2 and ZrO_2 catalysts, while nitridation was most effective for the Al_2O_3-based catalyst and less effective for ZrO_2.

The spent catalysts separated after each experiment were analysed by an identical set of methods to help in the discussion of the effect of reaction conditions and vegetable oil addition on the product properties. Table 4 summarizes the results of characterization of all the spent catalysts.

All the catalysts used in catalytic screening showed decreases in the contents of the main support and molybdenum (as the active phase marker). On the other hand, all these catalysts showed significant contents of carbon in their structures. Carbon originated in the samples from two sources. The first source is the contamination of the catalyst sample by the fine particles of SiC which is used in catalyst dilution, and the second one is the carbon depositing by coking during the experiment. The highest carbon content was detected in $MoCx/Al_2O_3$ and both the ZrO_2-supported catalysts. In the case of $MoCx/Al_2O_3$, carbon originated from the deposition of coke in the catalyst bed, whereas, in the case of the ZrO_2-supported catalysts, the effect of SiC contamination was much higher. Although these catalysts were contaminated with an inert material, the decrease in the specific surface area was mainly attributed to the formation and deposition of coke in the catalyst bed. The change in the ratios of the support metal precursor to molybdenum was reflected in the reduced molybdenum contents of the spent catalysts. The molybdenum loss was attributed to the attrition of the catalyst during its removal from the reactor by vacuum cleaning. The catalyst, after separation from the mixture, mainly consisted of particles of sizes up to approximately 400 μm.

The TiO_2-supported catalysts and the $MoNx/Al_2O_3$ catalyst showed increased sulfur contents of up to 1.18 wt%. Taking into account the fact that no sulfur was detected in the fresh catalysts, the sulfur detected after the experiment can be attributed to the AGO. The sulfane produced by the HDS reaction interacted with the residual molybdenum oxides and reduced molybdenum to the respective molybdenum sulfides. These reactions do not cause any problems to the desired reaction, because they occur on additional active sites in the system that have no negative impact.

Comparison of the pore-size distributions obtained by mercury porosimetry revealed that the ZrO_2-supported (Fig. 3e–f) catalysts and $MoCx/Al_2O_3$ (Fig. 3a) showed significant changes in the pore volume and the pore size distribution.

Regarding the elemental analysis, the porosimetry measurement revealed the loss of the porous structure of the ZrO_2-supported catalysts through either clogging by carbon deposits or collapse of the catalyst support. The pore volume of $MoCx/Al_2O_3$ significantly decreased owing to the carbon deposits, and the mean pore diameter decreased from 9 to 7 nm as a result of coking and partially as a result of the sulfiding of molybdenum and molybdenum oxide. $MoNx/Al_2O_3$ and the TiO_2-supported catalysts (Fig. 3b–d) showed lower decreases in the pore volume, which are in good agreement with the changes in the specific surface areas (Tables 3 and 4). The mean pore diameters of these catalysts were reduced 20% in comparison with the fresh catalysts (from 10 to 8 nm for $MoNx/Al_2O_3$, from 24 to 19 nm for the TiO_2-supported catalysts). The decrease in the mean pore diameter could be explained as an effect of the sulfur contained in the feedstock that interacted with the molybdenum and molybdenum oxides in the pores to form MoSx compounds [21].

3.2. Effect of operating conditions

The hydrotreatment of atmospheric gasoil was carried out at three different temperatures (330, 340 and 350 °C) and two different feedstock space velocities (WHSV = 1 and 2 h^{-1}), in order to study the effect of the operating conditions on the reaction products and the catalyst activity, i.e. HDS and HDN efficiencies.

Table 3
Characterization of fresh catalysts.

Catalyst	$MoCx/Al_2O_3$	$MoNx/Al_2O_3$	$MoCx/TiO_2$	$MoNx/TiO_2$	$MoCx/ZrO_2$	$MoNx/ZrO_2$
S_{BET}, m^2/g	142.6	148.6	102.1	103.7	107.1	117.5
Metal ICP-OES, %	–					
Mo	20.1	21.1	16.5	17.7	7.78	8.16
Al	36.7	40.0	–	–	–	–
Ti	–	–	44.5	43.9	–	–
Zr	–	–	–	–	57.5	57.8
sp*/Mo (wt/wt)	1.83	1.90	2.70	2.48	7.39	7.08
Elemental analysis, %	–					
C	1.02	0.14	1.06	0.42	0.49	0.16
N	0.05	0.78	0.16	0.53	0.05	0.21
Mo/C ratio	0.25	–	0.19	–	0.20	–
Mo/N ratio	–	0.34	–	0.42	–	0.49

* sp = support precursor metal.

Table 4
Characterization of spent catalysts.

Catalyst	$MoCx/Al_2O_3$	$MoNx/Al_2O_3$	$MoCx/TiO_2$	$MoNx/TiO_2$	$MoCx/ZrO_2$	$MoNx/ZrO_2$
S_{BET} [m^2/g]	8.3	115.4	70.3	54.9	25.4	7.4
Metals – ICP-OES (%)	–					
Mo	12.2	15.9	9.5	8.4	4.6	1.8
Al	25.7	34.4	–	–	–	–
Ti	–	–	38.7	29.2	–	–
Zr	–	–	–	–	38.2	14.3
sp^*/Mo (wt/wt)	2.11	2.16	4.07	3.48	8.30	7.94
Elemental analysis (%)	–					
C	24.1	6.69	3.65	4.75	10.90	16.60
N	0.05	0.54	0.18	0.37	0.05	0.05
S	0.21	1.18	0.72	0.39	0.05	0.09
Mo/C ratio	0.01	–	0.03	–	0.01	–
Mo/N ratio	–	0.37	–	0.28	–	0.46

* sp = support precursor metal.

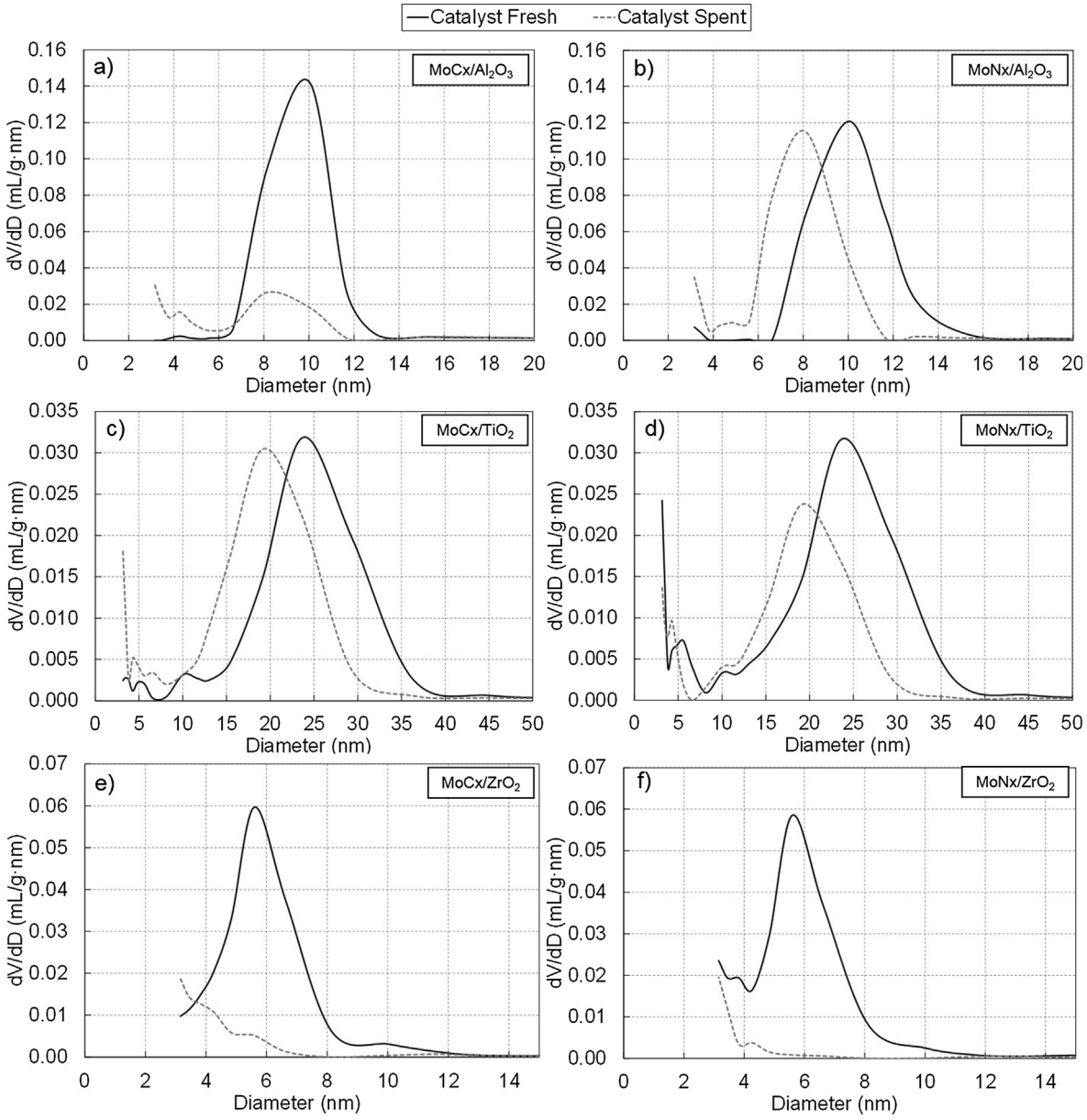

Fig. 3. Pore diameter distributions on different catalyst surfaces, as measured by mercury porosimetry.

3.2.1. Reaction products

The first part of the analysis of the results involved the determination of the mass balances for each experiment after taking into account the feedstocks and the corresponding products obtained, namely liquid and gaseous. Table S1 of the Supplementary data shows the mass balance results for the carbide and nitride catalysts with Al_2O_3, TiO_2 and ZrO_2 supports. The 'Mass closure', defined as the ratio between the total outputs and the total inputs multiplied by 100, was > 96% in all the cases, with the average being 97.7 ± 0.84% (calculated for all the experiments). This pointed to good mass balancing and a high reproducibility of the results. The errors were mainly attributed to the losses of the liquid during sampling and to the use of a low-accuracy gas flow meter (off-gas line).

Simdis was performed for general characterization of the liquid products. Identical boiling point distributions were observed for the reaction temperatures 330–350 °C. A similar profiles of the paraffins were obtained independently of the reaction temperature or WHSV used for all the catalysts tested. Fig. S1 of the additional data shows, as an example, the paraffin profile of desulfurized gasoil at different operating conditions with $MoCx/Al_2O_3$ and $MoNx/Al_2O_3$ catalysts. The gaseous products were identified by GC-RGA and quantified with an off-gas flow meter. The main off-gas component was H_2 in concentration of 98–99 vol%. The other compounds were C_1–C_3 light hydrocarbons (i.e. methane, ethane and propane). In this sense, the main gaseous product identified was methane, with its amount being in the range 65–75 vol%. However, this amount was distorted owing to its presence in the fresh H_2 stream (refinery quality, 99.5 vol% H_2). Its formation was attributed to the demethanization reactions and minor cracking of the feedstock. The role of the reaction conditions pointed to slight increases in the amounts of propane and ethane as the temperature rise from 330 to 350 °C; on the other hand, the methane concentration remained practically the same or experienced a slight reduction. On the other hand, the decrease in the WHSV from 2 to 1 h^{-1} resulted in an increase in the methane concentration, with corresponding decreases in the concentrations of the remaining gaseous products. These results are in good agreement with the expected results, because a light cracking phenomenon is commonly associated with middle distillate hydrotreatment [22].

The H_2 consumption and light gas production could be calculated on the basis of reaction off-gas analysis and completion of mass balance. The propane present displayed the clearest behaviour, according to the operating conditions used. Fig. 4 shows the hydrogen consumption and propane production in grams per kilogram of feedstock processed as functions of the reaction temperature (330–350 °C) and the WHSV (1, 2 h^{-1}).

Significant differences were observed in the hydrogen consumption and the formation of gaseous products, depending on the active phase and catalyst support selected. When Al_2O_3 was used as the catalyst support, no significant impact of active phase selection was observed. Only at the reaction temperature of 350 °C did the $MoCx/Al_2O_3$ catalyst show a significantly lower hydrogen consumption compared to that at 340 °C. Together with the changes in the porosity and the specific surface area, the increase in the reaction temperature beyond 340 °C was identified as the reason for catalyst deactivation. $MoNx/Al_2O_3$ showed an increasing trend of H_2 consumption with increasing reaction temperature, while the amount of propane formed was constant across the three reaction temperatures. The concentration of the propane formed over the Al_2O_3-supported carbide showed an increase after the reaction temperature was increased to 340 °C, however, further increase in the temperature did not increase the propane yield further owing to the deactivation described earlier.

For the TiO_2- and ZrO_2-supported catalysts, increases in the H_2 consumption with increasing reaction temperature were observed. For both these supports, the conclusion of higher catalytic activity of the active carbide phase can be correlated with the H_2 consumptions. The propane production pointed to constant yields, without any effect of the reaction temperature in the range 330–350 °C, over the TiO_2 catalyst support, indicating low sensitivity of the catalyst to cracking in this temperature range. Both the ZrO_2-supported catalysts showed significant increases in the concentrations of the propane formed after the temperature reached 340 °C. At lower reaction temperatures, no propane was detected in the reaction off-gas. The H_2 consumption decreased after increasing the reaction temperature to 340 °C for $MoNx/ZrO_2$, which showed catalyst deactivation followed by an increase in the activity at 350 °C. As in the case of $MoCx/Al_2O_3$ catalyst, that behaviour could be explained by the equilibrium of hydrogenation/dehydrogenation of AGO molecules during the hydrotreatment. However, a complete molecular analysis is necessary to confirm it.

Similar to conventional sulfided catalysts [23], most of the tested catalysts showed higher H_2 consumptions at a lower WHSV. The increased consumptions were 1.5–2.3 times the amount of H_2 consumed at 330 °C and 2 h^{-1}. The exceptions were the $MoNx/TiO_2$ and $MoCx/ZrO_2$ catalysts. This fact can be attributed to the combination of HDS and HDN reactions being preferred over the hydrogenation of unsaturated compounds (more details in the following section). In the same way, at the lower WHSV, most of the catalysts tested showed increases in light gas productions, particularly propane production. This fact could suggest an increase in the cracking activity of the catalyst under these operating conditions. An exception to this behaviour was observed in the case of $MoCx/TiO_2$ catalyst, which showed higher cracking activity at 2 h^{-1} WHSV.

3.2.2. Product properties

Significant changes in the variables of the operating conditions (reaction temperature 330–350 °C, WHSV = 1 and 2 h^{-1}) modified the characteristics of the desulfurized gas oil. The most important changes were observed in the densities of the liquid products. Fig. 5 shows the effects of temperature and WHSV on the density at 20 °C.

The liquid product density decreased with increasing reaction temperature for all the catalysts tested. Based on the catalyst support used, the product densities generally increased in the order $Al_2O_3 < TiO_2 < ZrO_2$. Similar results were observed when the space hourly velocity was changed from 2 to 1 h^{-1}. The Al_2O_3 and TiO_2 catalysts showed increases in the densities with increasing space velocity, whereas the ZrO_2 catalyst revealed a slight reduction in the density. As shown by the Simdis curves of Fig. S1, the decrease in density cannot be clearly attributed to the cracking of the feedstock into lighter hydrocarbons. The decrease in the product density can be explained as an effect of the hydrogenation reactions of the feedstock, as well as by the typical reduction of the specific weights of the compounds through double bond saturation or heteroatom removal from the structure during hydrotreatment.

No significant changes were observed during elemental analysis (C and H %) or in the acidity index of the desulfurized gasoil. However, important changes were observed in the bromine index of the liquid products as a result of the saturation of the double bonds, due to the effect of the operating conditions. Fig. 6 shows the bromine index for each catalyst at the different operating conditions used in this study.

The bromine indices determined showed trends that were different from those of the product densities measured. Excluding the $MoCx/Al_2O_3$ catalyst, the bromine index increased upon increasing the reaction temperature from 330 to 340 °C, and then decreased as the temperature was further increased to 350 °C. This behaviour was not in agreement with the generally expected results, where by a higher reaction temperature results in a significant decrease in the bromine index for the most of the catalysts [24]; this discrepancy was particularly accentuated for the Al_2O_3 and TiO_2 supports investigated in this study. As noted earlier, an exception to the observed trends was $MoCx/Al_2O_3$, where a significant decrease in the bromine index was observed due to saturation after the reaction temperature increased from 330 to 340 °C. The trends in the bromine index, with a maximum or minimum at 340 °C, are determined by catalyst deactivation after the reaction

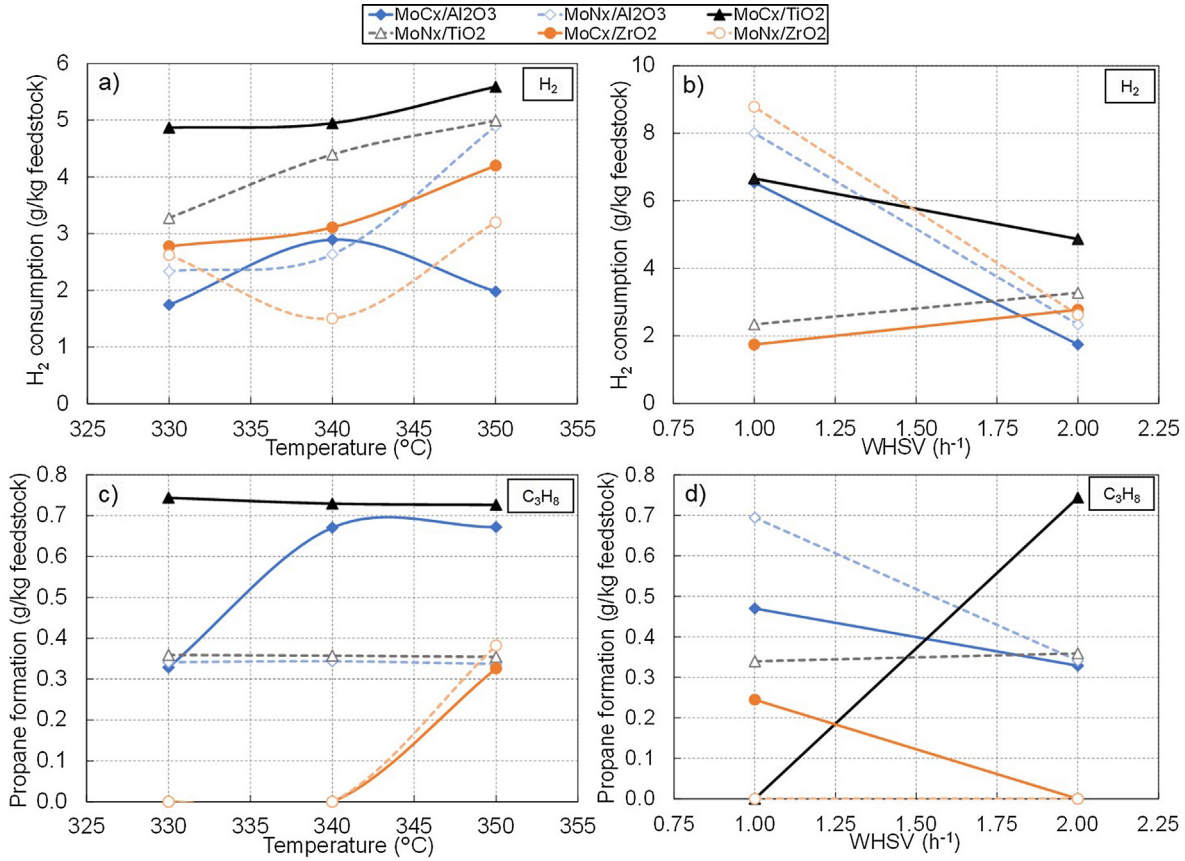

Fig. 4. Hydrogen consumption and propane production at different operating temperatures and WHSVs.

temperature increases. Additionally, hydrogenation can be understood to be a competitive reaction to the HDS and HDN reactions [25], which are usually promoted when the reaction temperature is increased in the range 320–430 °C; on the other hand, the saturation of the double bonds in the linear chains and aromatic compounds is typically slowed down thermodynamically upon increasing the reaction temperature [26–28]. Thus, the HDN and HDS reactions are preferred on the active sites and the hydrogenation activity of the double bonds is reduced. This can explain the unexpected decrease in the H_2 consumption over MoCx/Al_2O_3 at 350 °C (Fig. 4a), which was a result of the reduction in the hydrotreatment activity in favour of the HDS and HDN reactions (Fig. 7).

Similarly, a decrease in the feed rate (WHSV) resulted in significant decreases in the bromine indices of MoCx/Al_2O_3, MoNx/Al_2O_3, MoNx/TiO_2 and MoCx/ZrO_2 catalysts relative to the conventional catalyst [23]. On the contrary, MoCx/TiO_2 and MoNx/ZrO_2 catalysts showed increases in the bromine index at the lower space velocity. This atypical behaviour was attributed to the problem of accessibility to the active sites and mass transfer limitations as a result of the low specific surface areas and the changes in the porous structures of the catalysts. The products derived from the hydrotreatment of AGO or AGOR could block the active sites of the reactants at the lower WHSV, thus decreasing the catalytic activity. A higher feed rate and faster flow of the gaseous and liquid reactants could shift the reaction closer to the kinetic regimen, thereby promoting the accessibility to the active sites for hydrotreatment, as confirmed by the increased H_2 consumption (Fig. 4b). Thus,

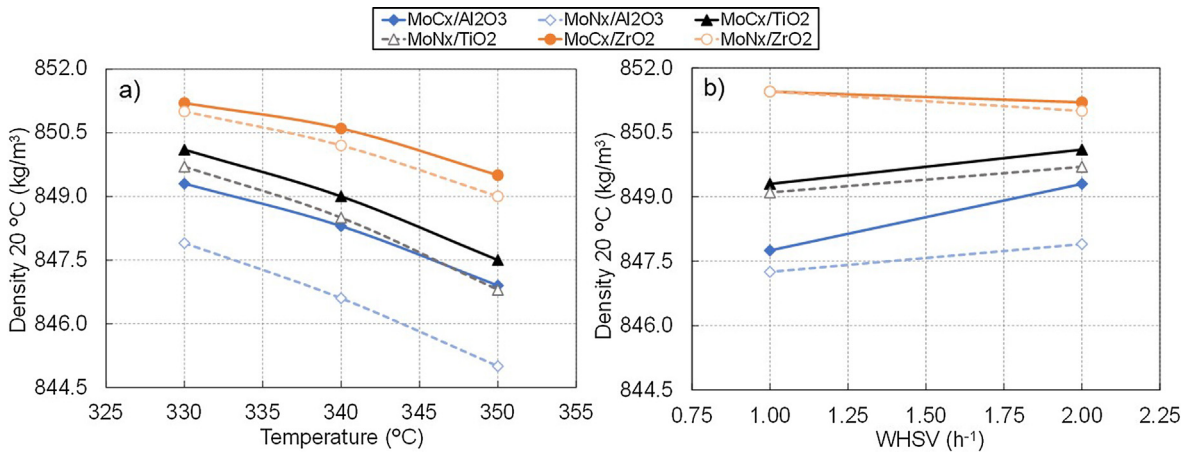

Fig. 5. Density at 20 °C for different operating temperatures and WHSVs.

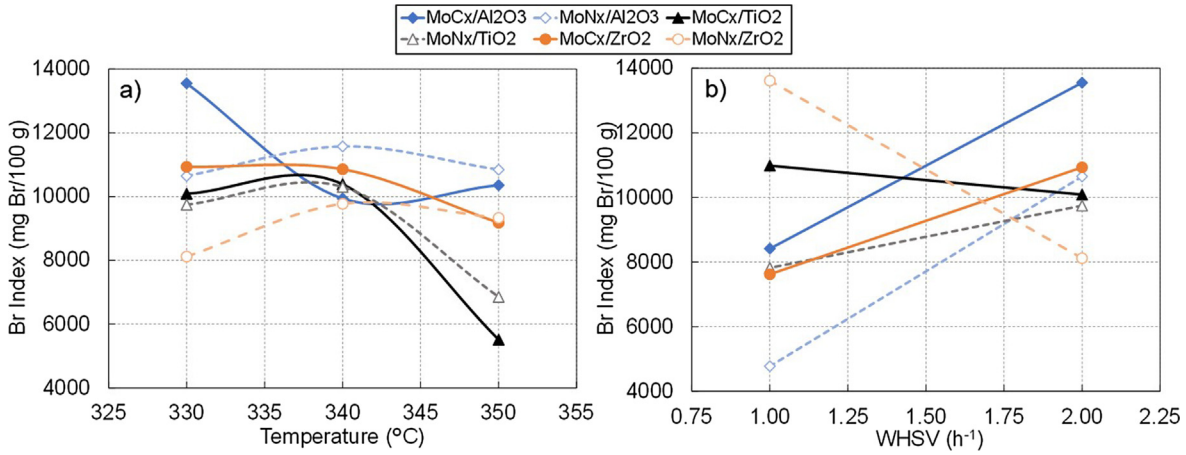

Fig. 6. Bromine indices obtained at different temperatures and WHSVs.

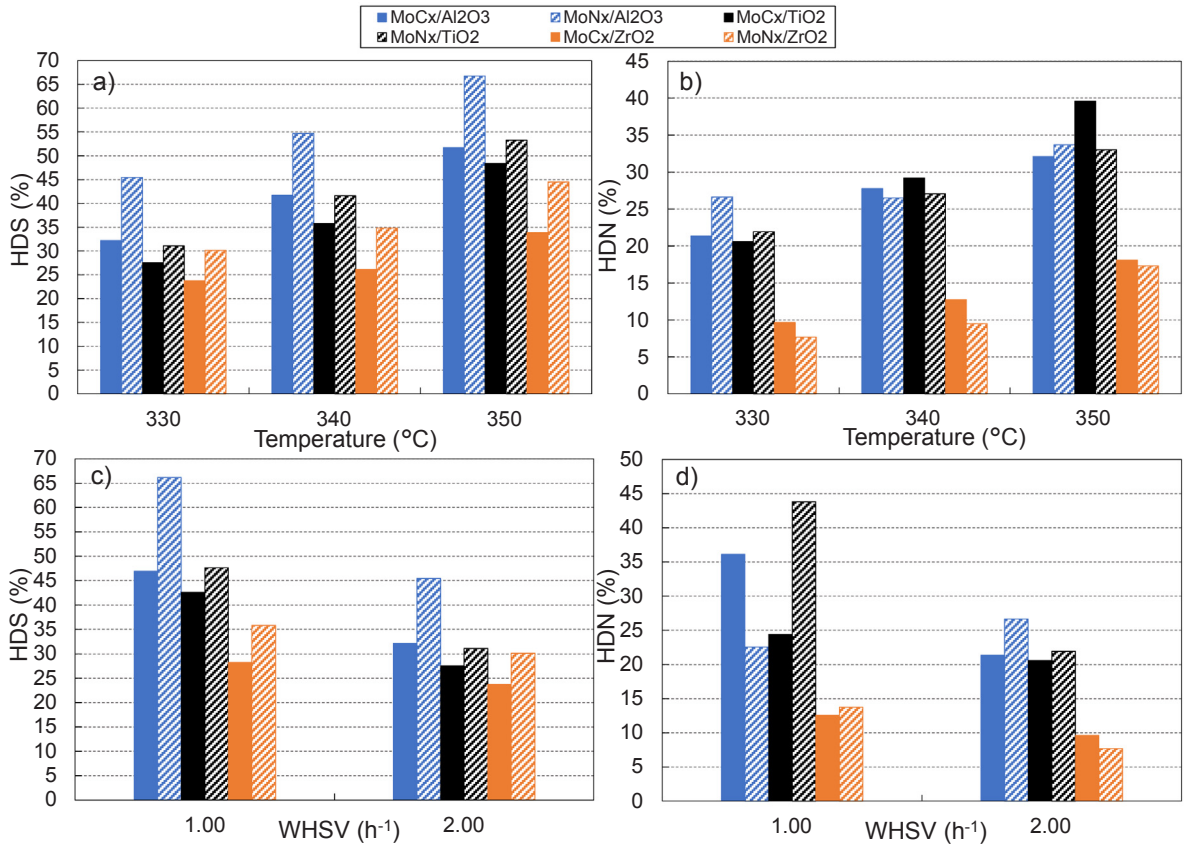

Fig. 7. HDS and HDN efficiencies obtained at different operating conditions.

the unexpected behaviour of $MoCx/TiO_2$ catalyst can be explained by the reduced accessibility to the active sites, which is similar to the case of $MoNx/ZrO_2$, in combination with the reduced HDS activity which slightly increases the potential for the hydrogenation reactions to occur.

3.2.3. HDS and HDN efficiencies

The sulfur and nitrogen contents of hydrotreated middle distillates and gas oils are the most important process parameters. According to EN 590, the maximum limit of 10 ppm of sulfur content puts high pressure on the process and the catalyst properties. As sulfided catalysts are capable of fulfilling this requirement, their alternatives must also be of the same or higher quality. In this sense, HDS and HDN efficiencies can be used as quantitative parameter for catalyst activity comparison.

The HDS and HDN activities were calculated at all the stages of the experiments. Fig. 7 shows the comparison of the HDS and HDN efficiencies obtained at different operating conditions for all the catalysts tested.

All the catalysts showed increases in both HDN and HDS efficiencies with increasing reaction temperature, which is in good agreement with the reported behaviour of commercial catalysts [10]. Generally, it is possible to claim that MoNx catalysts showed higher efficiencies during the HDS reaction than the MoCx types. The HDN efficiencies revealed less significant differences between the MoCx and MoNx catalysts and, especially at the temperatures 340 and 350 °C, the MoCx catalysts were found to be slightly more active towards denitrification. Furthermore, in all the cases, the HDS efficiency was always higher than the HDN

efficiency. Comparing the catalytic supports, Fig. 7a, b shows that the most active catalysts were the ones that used Al_2O_3 as the support, while the least active catalysts were the ZrO_2-based supports. These results pointed to $MoNx/Al_2O_3$ being the most active catalyst, exhibiting almost 70% sulfur removal when tested for AGO hydrotreatment, although $MoCx/TiO_2$ showed the highest HDN efficiencies at 340 and 350 °C.

The role of feed rate in the HDS and HDN activities is shown in Fig. 7c, d by comparing the HDS and HDN efficiencies of AGO hydrotreatment over the studied catalysts at different WHSVs. Based on the H_2 consumption, the decrease in the WHSV to $1\,h^{-1}$ resulted in significant increases in the HDS activities, which were in the range 5–20%, depending on the catalyst used. At the WHSV of $1\,h^{-1}$, $MoNx/Al_2O_3$ showed the highest HDS activity, followed by $MoCx/Al_2O_3$ > $MoNx/TiO_2$ > $MoCx/TiO_2$ > $MoNx/ZrO_2$ > $MoCx/ZrO_2$. Similarly, the $MoCx/Al_2O_3$, TiO_2 and ZrO_2 catalysts showed increases in their HDN activities with WHSV reduction, which were in the range 4–22%, depending on the catalyst. However, $MoNx/Al_2O_3$ catalyst displayed a reduction in its HDN activity, decreasing from 19.0% to 14.9%. This could be explained by the slight deactivation of the catalyst during the progress of the experiment.

The molybdenum carbide and nitride catalysts exhibited significant activities, based on their HDS and HDN efficiencies. This was correlated with the studies of Refs. [13,27], which demonstrated that molybdenum carbide and nitride catalysts were capable of absorbing hydrogen and transferring them to the molecules of middle distillates during the hydrotreatment reactions. Thus, optimization of the operating conditions led to significant improvements in the HDS/HDN activities.

3.3. Effect of vegetable oil addition

The co-processing of three different mixtures of AGO and RSO (5, 10 and 25 wt%) was performed at 330 °C and 5.5 MPa to study the products formed, their influence on the fuel properties and on the catalytic activity.

3.3.1. Reaction products

Based on previous experiments on co-processing with conventional sulfur $NiMo/Al_2O_3$ catalysts [10], the addition of RSO (food quality grade) would increase the paraffin character of desulfurized gas oil. Analogous to Section 3.2, Table S2 of Supplementary data shows the mass balance results for the carbide and nitride catalysts with Al_2O_3, TiO_2 and ZrO_2 supports. In this case, the mass closures of AGO/RSO co-processing balances were higher than 96%, with the average being 97.2 ± 0.7% for all the catalysts used. As mentioned in the introduction section, during hydrotreatment, the triglyceride feedstock was converted into HVO, which was the main product, and light gases (mainly CO, CO_2 and C_3H_8) and liquid water, which were the by-products. As a result of vegetable oil addition, the organic product output decreased, while those of the gaseous products increased.

Using the mass balance data of the co-processing stages and AGO hydrotreatment at 330 °C, it was possible to determine the yields of the main reaction products obtained during the RSO co-processing for each catalyst according to the equation:

$$\text{Product yield} = \frac{\text{Product formed } (g)}{\textit{Vegetable oil in feedstock } (g)} \cdot 100 \quad (3)$$

where the 'product formed' only refers to the mass of that reaction product (HVO, water or light gases) formed from the RSO hydrotreatment, and 'vegetable oil in feedstock' represents only the mass of RSO used during the corresponding co-processing stages. Table 5 summarizes the yields of HVO, water and light gases from RSO co-processing for each of the catalysts tested.

These yields had mass closures slightly lower than those presented in Tables S1 or S2, with the average being 93.1 ± 1.7 wt%, which is still a good result. Water production was observed only in the liquid samples as a result of the co-processing of 10 and 25 wt% RSO. The amount of this side-product was typically up to 3 wt%. For such amounts, it was not usually possible to separate the water quantitatively owing to its dispersion in the form of small drops at the bottom of the sampling vessel, therefore, this phenomenon probably increased the organic yield. The main product, 88.5 ± 1.0 wt% of co-processed RSO, was a mixture of paraffins, mostly with carbon numbers 15–18 and containing traces of olefins and isoparaffins. The distribution of paraffin carbon numbers and the distribution of gaseous products were influenced by the selectivity of the reaction mechanism and the reaction pathway, respectively. The preference in reaction mechanism was determined by a combination of the catalyst type and the reaction conditions during triglyceride hydrotreatment. On the other hand, light gases (mainly methane, carbon oxides and propane) showed yields in the range 2.0–5.5 wt%, depending on the catalyst used. In this sense, the ZrO_2 catalysts yielded less gases, which is a result of their lower activity towards hydrotreatment.

Table 5
Product yields from AGO/RSO co-processing at 330 °C and 5.5 MPa.

Experiment no.	Catalyst	RSO (wt%)	HVO (wt %)	Water (wt%)	Light gases (wt%)	Mass closure (%)
1	$MoCx/Al_2O_3$	5–10–25	89.7	1.1	4.7	95.5
2	$MoNx/Al_2O_3$	5–10–25	89.3	0.0	4.7	94.0
3	$MoCx/TiO_2$	5–10–25	88.0	1.1	5.4	94.5
4	$MoNx/TiO_2$	5–10–25	86.8	0.0	5.1	91.9
5	$MoCx/ZrO_2$	5–10–25	89.4	0.0	2.1	91.5
6	$MoNx/ZrO_2$	5–10–25	87.8	0.0	3.3	91.1

The paraffinic nature of HVO and the presence of paraffins in the studied AGO allowed the study of the deoxygenation mechanism by using Simdis analysis. Specific peaks in the Simdis chromatogram could be used to simply visualize the main deoxygenation products. The analytical data were exported in detail by using improved settings in GC operating SW and numerically derived to obtain a chromatogram with relative (normalized) signal intensities. Fig. 8 shows a complex comparison of the Simdis analysis of different amounts of the samples of RSO co-processed over all the catalysts investigated. The amount of RSO co-processed varied from 0 to 25 wt% in AGO. The main paraffins, namely n-C_{18}, n-C_{17}, n-C_{16} and n-C_{15}, as well as the intermediate products, have been identified and marked in Fig. 8.

Octadecane (n-C_{18}), the product of the C_{18} alkyl groups of the triglycerides hydrodeoxygenated, was identified as the dominant product of the co-processing in all the experiments. The peak at the boiling points of 317–320 °C (Fig. 8) shows a gradual increase in the maximum intensity with increasing content of RSO in the feedstock. The heptadecane (n-C_{17}) peak at the boiling points of 302–304 °C did not increase in intensity as much. A significant increase in the n-C_{17} peak intensity was observed only in the case of 25 wt% RSO co-processing over $MoCx/Al_2O_3$ catalyst. This pointed to the occurrence of major HDO reaction and minor selectivity to the HDC reaction mechanism at 330 °C for all the catalysts studied. These results are in good agreement with those of Sousa et al. [18] and Qin et al. [29]. They studied the hydrotreatments of different vegetable oils (such as sunflower oil and RSO) over β-Mo_2C/Al_2O_3 and Mo_2C/carbon nanofiber catalysts, respectively. These results are also in concordance with the reaction selectivity observed over the conventional commercial sulfide $NiMo/Al_2O_3$ catalyst used in the vegetable oil co-processing at 320 °C [10]. The HDO pathway is desirable for yielding the maximum possible amounts of HVO and waste water, as a by-product. On the other hand, the dominant decarboxylation reaction pathway involving minimal CO_2 reduction could hardly reduce the H_2 consumption. Nevertheless, the reduction of CO_x into methane is preferred in order to avoid problems due to corrosion,

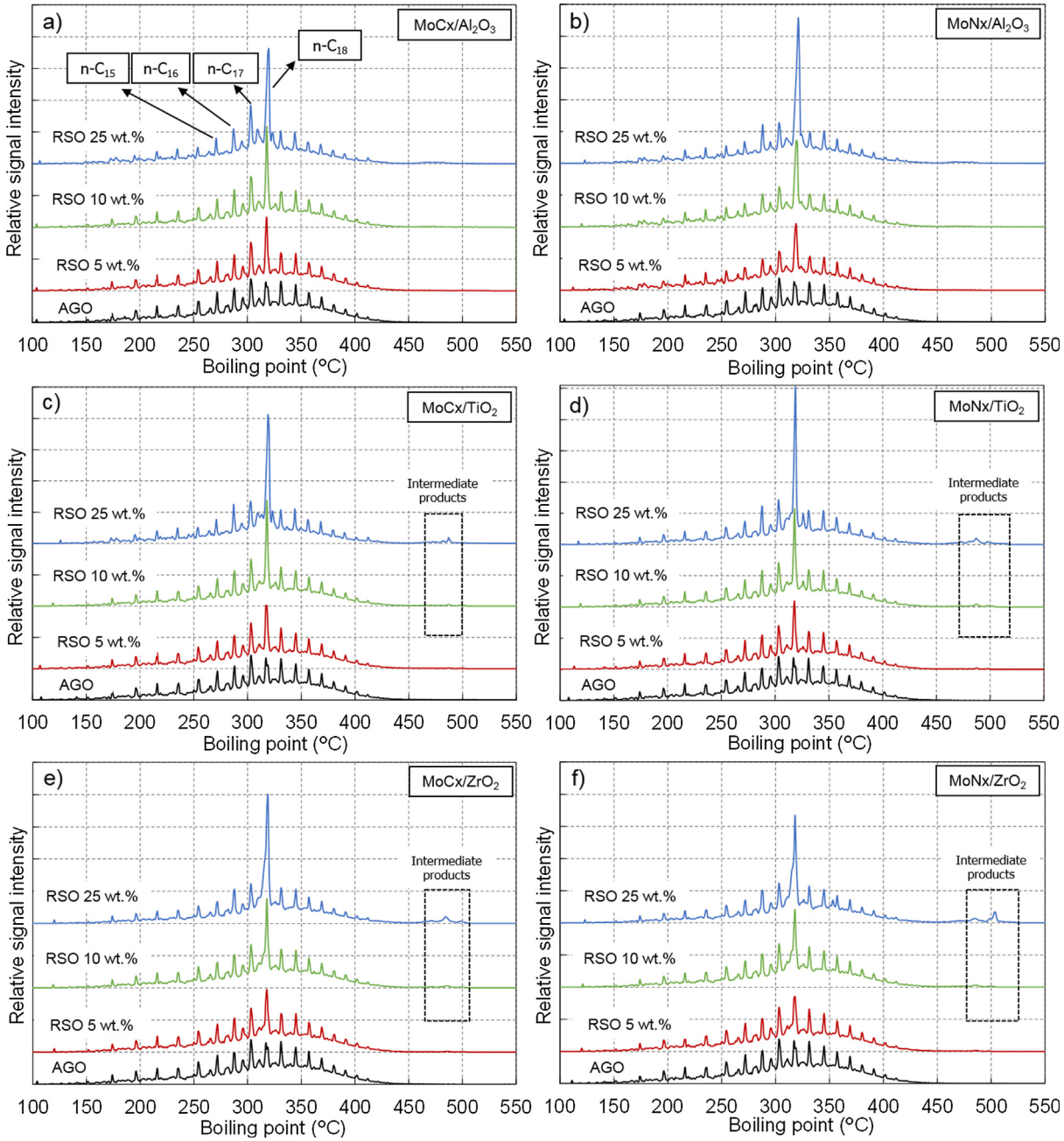

Fig. 8. Simdis results of AGO/RSO co-processing.

particularly at high pressures [30].

The co-processing of 10–25 wt% RSO over TiO_2- and ZrO_2-supported catalysts resulted in the formation of clear products with white solid particles (or 'waxes' [11]), which melted after heating the samples above 50 °C. These molecules were identified as the intermediate products of triglyceride deoxygenation. The presence of minor peak(s) in Simdis analysis with boiling points in the range 460–520 °C (detected for 10–25 wt% co-processing over ZrO_2- and TiO_2-supported catalysts; Fig. 8c–f) pointed to the existence of large esters of intermediate fatty acids and alcohols, or diesters of propanediols, respectively. Calibration for a more accurate identification was not possible. The presence of waxes in the products of 25 wt% RSO co-processing might be attributed to saturated carboxylic acids, which are another deoxygenation intermediate. Fatty acids were identified based on the group of peaks observed in the approximate boiling point range 345–380 °C. However, the presence of these compounds was not confirmed by Simdis.

Similar to the AGO hydrotreatment, H_2 was the main off-gas compound, with concentration in the range 98–99 vol%. The main gaseous products formed during the co-processing reactions were light gases such as CO_2, CH_4, C_2H_6 and C_3H_8. Fig. 9 shows the H_2 consumptions and light gas productions (in grams per kilogram of feedstock processed) as functions of RSO concentration at 330 °C and 2 h^{-1} WHSV (results at 0 wt% of RSO correspond to the AGO-100 wt% hydrotreatment).

The effect of increasing the content of RSO in the feedstock was an increase in the production of propane. This gas is the by-product of triglyceride deoxygenation, and is formed from the glycerol part of the ester molecule. The amount of propane increased linearly in the case of $MoNx/Al_2O_3$ catalyst (Fig. 9b), but, in the case of $MoCx/Al_2O_3$, the rate of increase was slightly lower at 25 wt% co-processing relative to those observed in the range 0–10 wt%. This could simply be a result of a deviation in the measurement, but similar trends were exhibited by

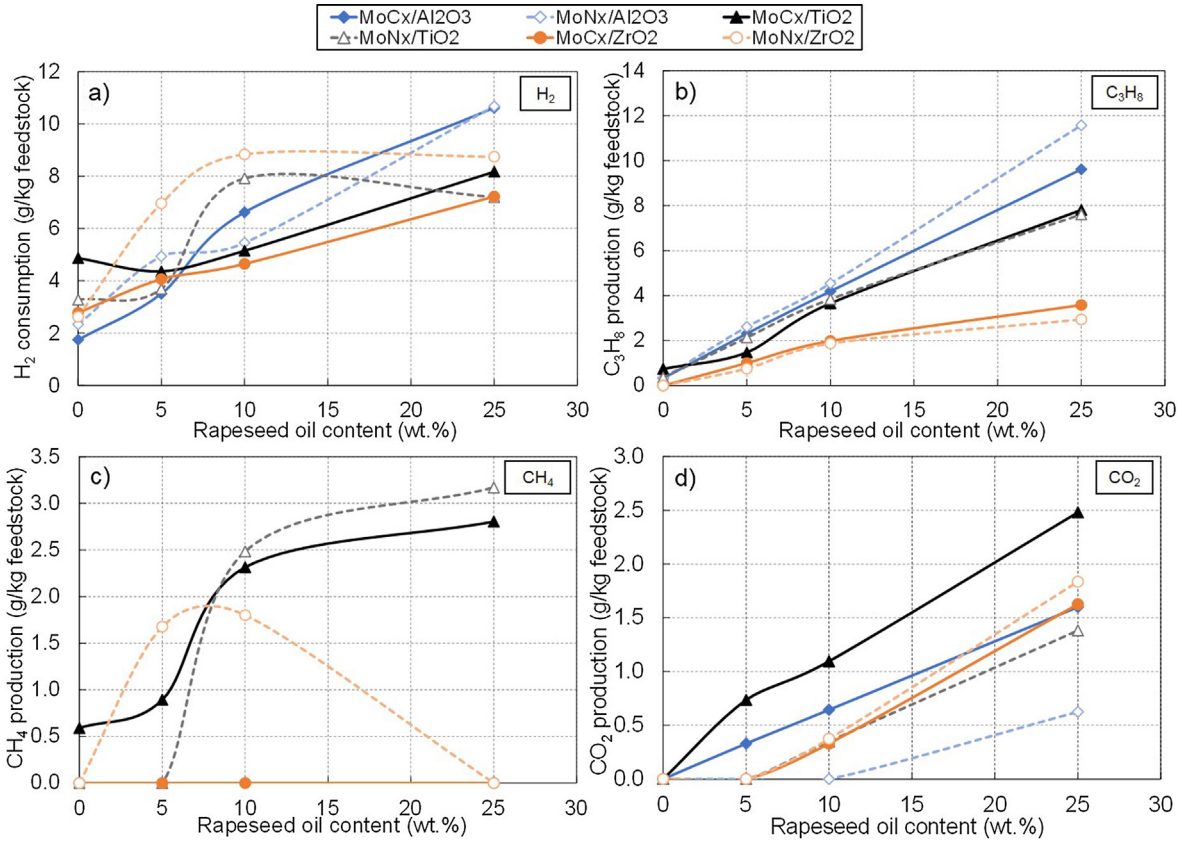

Fig. 9. H_2 consumption and light gas productions per kilogram of feedstock during AGO and RSO co-processing at 330 °C, 5.5 MPa, 2 h^{-1} WHSV (result at 0 wt% of RSO correspond to the AGO-100 wt% hydrotreatment).

other catalysts. Taking into account the Simdis analyses discussed earlier, this trend confirms the presence of partially decomposed triglycerides in the products of co-processing hydrotreatment. Incomplete conversion of glycerides, which are a partially fixed glycerol part of the feedstock, in the products resulted in the non-linear trend being observed for the propane production as a function of RSO content of the feedstock. The concentration of CO_2 is an important parameter of triglyceride deoxygenation, and reveals the ability of the catalyst to reduce CO_2 into methane. In all the cases, the CO_2 production increased linearly with increasing RSO content of the feedstock (Fig. 9d).

The H_2 consumption increased with increasing amount of RSO in the feedstock, but the consumption trends were not linear. The dependence of H_2 consumption on RSO concentration was governed by several factors. The parameter was calculated by using a set of measurements, each with a specific accuracy, and the selectivity towards the deoxygenation mechanisms can change depending on the RSO concentration, while the catalyst was not active enough to convert such a high amount (25 wt%) of RSO in the feedstock at the reaction conditions considered. The impact of low catalytic activity was significant in the case of MoNx/ZrO_2, with a slightly lower H_2 consumption observed for 25 wt% RSO than for 10 wt% RSO hydrotreatment. This was caused by too low a catalyst activity which resulted in incomplete conversion of triglycerides, as shown by the Simdis (Fig. 8) and propane production (Fig. 9) results. The low catalyst activity resulted in near zero activity towards CO_2 methanation, as well as minimal CH_4 production. Even though the CO_2 production was low, it has to be taken into account in future research, owing to its effect on the activity of the conventional catalyst of HDS/HDN (CoMo/Al_2O_3) during gasoil hydrotreatment [31].

3.3.2. Product properties

As the HVO is mainly composed of linear paraffins (n-C_{15} to n-C_{18}),

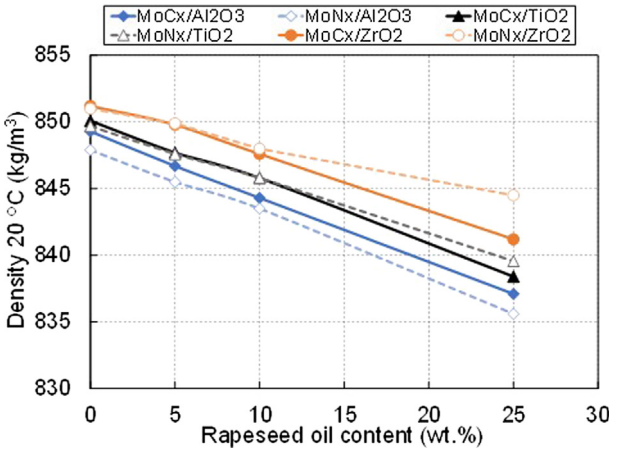

Fig. 10. Density measured at 20 °C for the co-processing of different AGO/RSO mixtures (result at 0 wt% of RSO correspond to the AGO-100 wt% hydrotreatment).

the co-processing of vegetable oil with AGO strongly affects the physical parameters of the product. Typically, the low density of paraffins caused a significant decrease in the densities of the products of co-processing. Fig. 10 shows the densities obtained at 20 °C of the products of co-processing for different amounts of RSO added to the AGO feedstock.

As expected, the density decreased linearly with RSO addition for most of the catalysts, and the effect of the RSO addition was much more significant than the effect of increasing the temperature. Similar to the results presented in Fig. 5, lower densities were obtained for MoNx/Al_2O_3, with the other catalysts following the order MoCx/

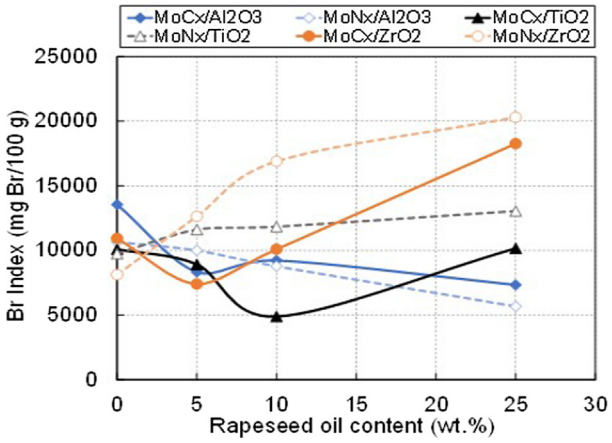

Fig. 11. Bromine indices of the co-processing of different AGO/RSO mixtures (result at 0 wt% of RSO correspond to the AGO-100 wt% hydrotreatment).

Al_2O_3 > MoCx/TiO_2 > MoNx/TiO_2 > MoCx/ZrO_2 > MoNx/ZrO_2. Different trends were observed in the case of 25 wt% RSO co-processing over MoNx/ZrO_2 catalyst. The incomplete conversion resulted in increased content of oxygenates, which increased the density of the hydrotreated product. Similar but not so significant behaviour was also observed in the case of MoNx/TiO_2 catalyst.

The elemental analysis results were not significantly affected by the addition of RSO to the feedstock. The average values of carbon and hydrogen contents were 86.5 and 13.5 wt%, respectively (the oxygen content was not determined). Similar behaviour was observed with the acidity index, with values being in the range 0.01–0.03 mg KOH/g. MoNx/ZrO_2 catalyst was an exception to this trend, displaying a significant increase in the acidity index up to 0.42 during the AGO/RSO 75/25 co-processing. This was a result of the incomplete conversion and the presence of carboxylic acids as intermediates. In the same way, significant changes were observed in the bromine index during vegetable oil addition. Fig. 11 shows the bromine indices for different AGO/RSO ratios.

According to the SIMDIS results, the catalysts MoCx/Al_2O_3, MoNx/Al_2O_3 and MoCx/TiO_2 showed decreasing trends in their bromine indices, which indicated high conversions of the triglycerides with negligible or low concentrations of intermediate products. This observation was in line with the results described in the literature for the conventional NiMo/Al_2O_3 catalyst and heavy gas oil with used cooking oil as the feed [27]. On the other hand, the other catalysts with higher concentrations of intermediate products showed increases in their bromine indices during the co-processing, which was particularly accentuated at 25 wt% of RSO in the feedstock. This would also explain the increase in the acid number.

3.3.3. Catalytic activity during AGO/RSO co-processing

The deoxygenation reactions of RSO compete with the HDN and HDS reactions of AGO. The addition of RSO into the fossil material increased the concentration of heteroatoms that needed to be removed. In the system with a set of competitive reactions, the dominant (preferred) reaction could eliminate the other types of reactions. As the RSO is known to be more reactive than AGO, the elimination of HDS and HDN reactions presented an unacceptable level of risk in AGO conversion. To analyse the effect of vegetable oil addition on the catalytic activity, the HDS and HDN efficiencies were determined at each stage of the co-processing, from 0 to 25 wt%. Fig. 12 shows the variations in the HDS and HDN efficiencies during the AGO/RSO co-processing over each of the catalysts used.

RSO addition did not significantly decrease the HDS ratio for the Al_2O_3- and TiO_2-supported catalysts. In fact, a slight increase was observed during RSO co-processing (2–3% HDS efficiency increase), particularly at 5–10 wt% RSO addition. This increase was particularly significant in the case of MoCx/Al_2O_3 catalyst, with an increase of 13% observed for 25 wt% RSO co-processing. The MoNx/Al_2O_3 catalyst was found to be the most stable, from HDS point of view. Opposite to this observation, the ZrO_2-supported catalysts decreased their HDS activities during the RSO co-processing, thereby showing high sensitivity to RSO addition beyond 5 wt%.

Similar to the HDS activity, the HDN efficiency hardly increased after switching to RSO co-processing over Al_2O_3- and TiO_2-supported catalysts. This effect was the most significant for 5–10 wt% RSO addition in the case of the MoNx/TiO_2 catalyst. An exception to this effect was observed in the products obtained from the experiments involving MoNx/Al_2O_3 and ZrO_2-supported catalysts, which showed significant decreases in the HDN activities (the efficiencies also decreased) during the vegetable oil co-processing, with the maximum decrease being 13%.

Thus, in the cases of the MoCx/Al_2O_3 and TiO_2-supported catalysts, no significant negative effect of RSO co-processing on their activities during the reaction was observed, indicating that the catalyst activity was high enough to complete the triglycerides HDO/HDC reactions. In this sense, the only effect found was slight increases in the HDN and HDS efficiencies during the co-processing, which was affected significantly by the amount (percentage) of RSO co-processed. This behaviour was according to authors' previous experiments of triglycerides co-processing with conventional sulfide catalysts [10]. In brief, the MoNx/Al_2O_3 catalyst was found to be the best catalyst for AGO/UFO co-processing in this study from HDS point of view, and the MoCx/Al_2O_3 and MoNx/TiO_2 catalysts were found to be the most attractive for a significant increase of the HDS and HDN efficiencies during the RSO co-processing respectively, i.e. better HDS and HDN selectivity.

3.4. Catalyst deactivation

As described in Experimental section, each experiment was divided into nine sections. Sections 4 and 8 were added to the screening process to analyse the effects of higher reaction temperatures and RSO co-processing on the catalytic activity after returning to the initial (reference) operating conditions. Then, the catalytic activity was checked based on the basic properties such as the density at 20 °C and the HDS and HDN activities.

3.4.1. Product quality at the reference operating conditions

The densities of all the samples were determined. Thus, the study of its changes after operating at higher reaction temperatures and the co-processing stages, corresponding to the Sections 4 and 8, provided information on the possible changes in the catalytic activity. Fig. 13 shows the comparison of the densities for hydrotreated gasoil produced in the reference section (330/1), the section after operation at elevated reaction temperatures (330/2) and the section corresponding to the co-processing stages (330/3) for all the catalysts investigated.

No significant changes (in the form of rapid density increases) were observed when the reaction temperature increased, maintaining approximately the same values for the densities measured at 20 °C. An exception to this behaviour was MoCx/ZrO_2, which showed an increase in the product density. Another evaluation of the activity (330/3) showed an increase in the density of the products obtained over the MoNx/Al_2O_3, TiO_2- and ZrO_2-supported catalysts. This density increase can be indicative of possible catalyst deactivation. The only catalyst showing a stable density was MoCx/Al_2O_3.

3.4.2. Catalytic activity at the reference operating conditions

As the density is only an indicative parameter for comparing the deactivations, the HDS and HDN efficiencies were also compared for the reference and evaluation stages. Fig. 14 shows the HDS and HDN efficiencies corresponding to the different stages of evaluation of the catalysts.

Temperature increase or RSO addition did not significantly decrease

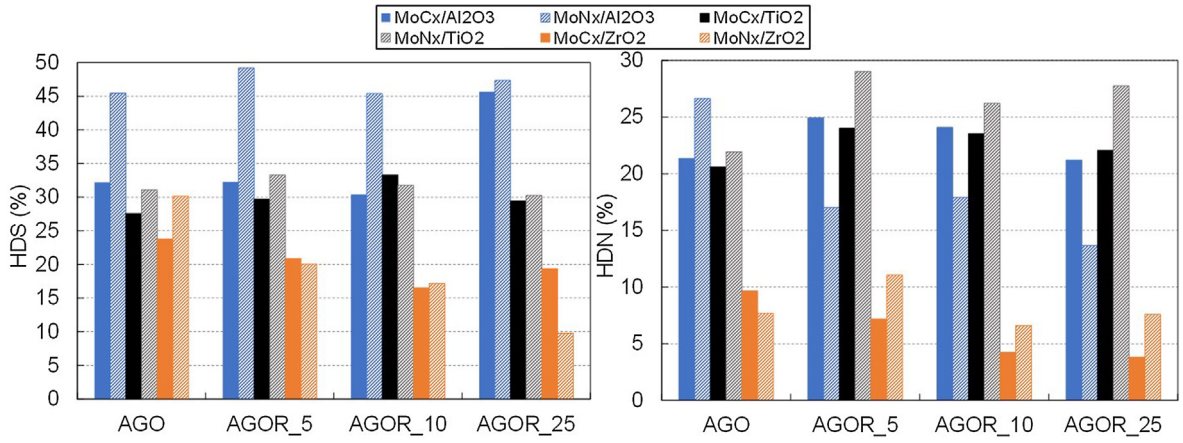

Fig. 12. HDS and HDN efficiencies determined for AGO/RSO co-processing.

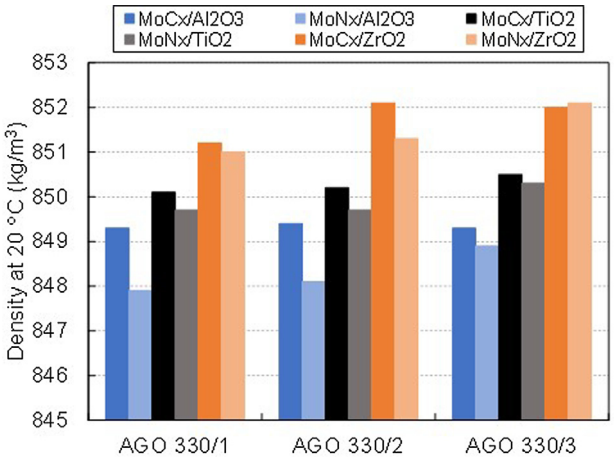

Fig. 13. Densities measured at 20 °C at different stages of evaluation of the catalysts.

the HDS activity. In fact, an increase was observed. These general increases in the HDS activity could be explained in terms of possible partial sulfidation of the catalyst surface [13,32], which resulted in the improvement in the HDS activity. The increases were 0.80, 2.35, 24.50, 3.70, 1.80 and 21.02 wt% for the carbide/nitride catalysts with Al_2O_3, TiO_2 and ZrO_2 supports, respectively. In accordance with the effect observed on the density, this increase in the HDS activity was lower in the evaluation stage 330/3, where a significantly reduced activity of $MoNx/ZrO_2$ catalyst was observed. This implied a higher impact of RSO addition on the catalytic activity than an increase in the operating temperature.

The HDN activity exhibited different behaviours, depending on the catalyst used. Therefore, after the temperature increase, the $MoCx/Al_2O_3$, $MoNx/TiO_2$ and $MoCx/ZrO_2$ catalysts showed increases of up to 2.50, 4.10 and 2.30 wt%, respectively. These represent significant improvements of their activities. However, the $MoNx/Al_2O_3$, $MoCx/TiO_2$ and $MoNx/ZrO_2$ catalysts revealed decreases in their activities, being up to 11.10, 0.70 and 1.10 wt%, respectively. RSO addition accentuated that effect for both the reactions. $MoCx/Al_2O_3$ showed the best behaviour, as it increased its HDN activity after the RSO co-processing.

The evaluation of the catalysts in two stages pointed to the positive effect of the increase in the reaction temperature on the low-temperature activity, as well as to the effect of vegetable oil addition on the catalyst tested. In general, the Al_2O_3- and TiO_2-supported catalysts studied did not reveal any significant negative effect on the HDS activity. Moreover, these results, together with the trends in H_2 consumption (Fig. 4) and the product bromine indices (Fig. 6) obtained at the different reaction temperatures, showed strong reversible $MoCx/Al_2O_3$ and $MoCx/TiO_2$ deactivations at temperatures above 350 and 340 °C, respectively.

4. Conclusions

Supported molybdenum carbide and molybdenum nitride catalysts (with Al_2O_3, TiO_2 and ZrO_2 as the supports) were tested and their properties determined during the hydrotreatment of AGO and its mixtures with triglyceride feedstock. Similar to conventional sulfide catalysts, an increase in the reaction temperature (from 330 to 350 °C) and a

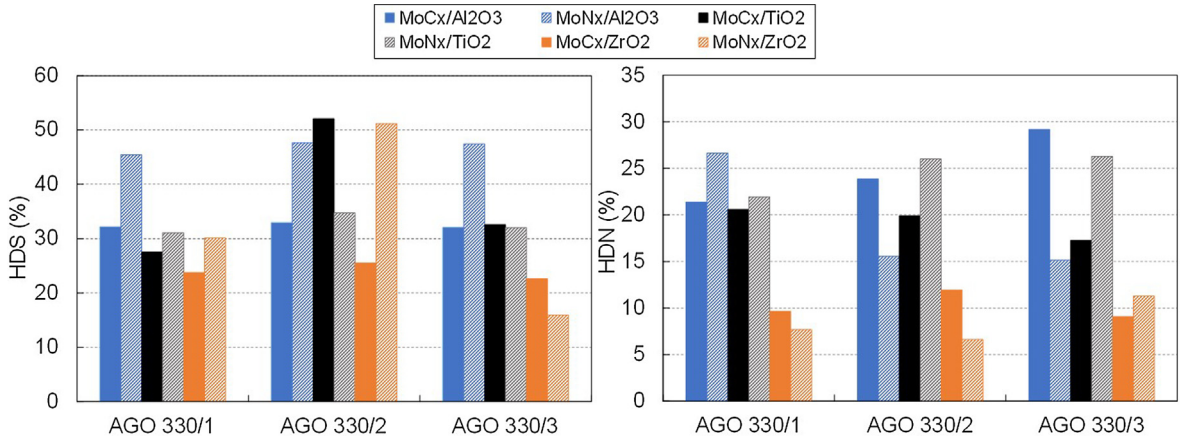

Fig. 14. HDS and HDN efficiencies determined at different stages of evaluation of the catalysts.

decrease in the feed rate (WHSV from 2 to 1 h^{-1}) resulted in significantly improved product properties (density, refractive index, bromine index) and higher HDS and HDN efficiencies. During the different co-processing stages, the hydrotreated RSO was converted into HVO, water and light gases (mainly propane and CO_2). Based on Simdis results, all the catalysts showed higher selectivities to the HDO reaction pathway than to the HDC reaction. An increase in the amount of linear paraffins (n-C_{16} and n-C_{18}) in the product resulted in changes in its properties, mainly in the density and bromine index. MoCx/Al_2O_3 showed the best behaviour for high levels of RSO addition, with slightly increased HDS and HDN activities. The MoNx/Al_2O_3 catalyst was identified as the most stable catalyst which did not exhibit any significant sensitivity to the increase in the reaction temperature or show any effect of RSO co-processing on the low-temperature activity. Al_2O_3- and TiO_2-supported molybdenum carbide and nitride catalysts were identified as candidates for further research in the field of alternative catalysts for the hydrotreatment of middle distillates.

Acknowledgements

This work is a result of the Development Project of UniCRE (project code LO1606), which was financially supported by the Ministry of Education, Youth and Sports of the Czech Republic (MEYS) through National Sustainability Programme I.

The results were obtained by using the infrastructure of the project Efficient Use of Energy Resources Using Catalytic Processes (LM2015039), which was financially supported by MEYS within the broader scope of large infrastructures.

Appendix A. Supplementary data

Supplementary data to this article can be found online at https://doi.org/10.1016/j.fuel.2019.05.165.

References

[1] Huber GW, Iborra S, Corma A. Synthesis of transportation fuels from biomass: chemistry, catalysts, and engineering. Chem Rev 2006;106:4044–98.
[2] Bezergianni S, Dimitriadis A. Comparison between different types of renewable diesel. Renew Sustain Energy Rev 2013;21:110–6.
[3] Al-Sabawi M, Chen J. Hydroprocessing of biomass-derived oils and their blends with petroleum feedstocks: a review. Energy Fuel 2012;26:5373–99.
[4] Kim SK, Han JY, Lee H, Yum T, Kim Y, Kim J. Production of renewable diesel via catalytic deoxygenation of natural triglycerides: comprehensive understanding of reaction intermediates and hydrocarbons. Appl Energy 2014;116:199–205.
[5] Jęczmionek L, Hydrodeoxygenation Porzycka-Semczuk K. decarboxylation and decarbonylation reactions while co-processing vegetable oils over a NiMo hydrotreatment catalyst. Part I: thermal effects – theoretical considerations. Fuel 2014;131:1–5.
[6] Bezergianni S, Dagonikou V, Sklari S. The suspending role of H2O and CO on catalytic hydrotreatment of gasoil; myth or reality? Fuel Process Technol 2016;144:20–6.
[7] Horáček J, Tišler Z, Rubáš V, Kubička D. HDO catalysts for triglycerides conversion into pyrolisis and isomerization feedstock. Fuel 2014;121:57–64.
[8] Bezergianni S, Dimitriadis A, Kalogianni A, Pilavachi PA. Hydrotreating of waste cooking oil for biodiesel production. Part I: effect of temperature on product yields and heteroatom removal. Bioresour Technol 2010;101:6651–6.
[9] Huber GW, Connor PO, Corma A. Processing biomass in conventional oil refineries: production of high quality diesel by hydrotreating vegetable oils in heavy vacuum oil mixtures. Appl Catal A-Gen 2007;329:120–9.
[10] De Paz Carmona H, Horáček J, Brito Alayón A, Macías Hernández JJ. Suitability of used frying oil for co-processing with atmospheric gas oil. Fuel 2018;214:165–73.
[11] Kubička D, Horáček J. Deactivation of HDS catalysts in deoxygenation of vegetable oils. Appl Catal A-Gen 2011;394:9–17.
[12] Bezergianni S, Dimitriadis A, Karonis D. Diesel decarbonization via effective catalytic Co-hydroprocessing of residual lipids with gas-oil. Fuel 2014;136:366–73.
[13] Furimsky E. Metal carbides and nitrides as potential catalysts for hydroprocessing. Appl Catal A-Gen 2003;240:1–28.
[14] Dolce GM, Savage PE, Thompson LT. Hydrotreatment activities of supported molybdenum nitrides and carbides. Energy Fuel 1997;11:668–75.
[15] Diaz B, Sawhill SJ, Bale DH, Main R, Phillips DC, Korlann S, et al. Hydrodesulfurization over supported monometallic, bimetallic and promoted carbide and nitride catalysts. Appl Catal A-Gen 2003;86:191–209.
[16] Da Costa P, Potvin C, Manoli JM, Genin B, Djéga-Mariadassou G. Deep hydrodesulphurization and hydrogenation of diesel fuels on alumina-supported and bulk molybdenum carbide catalysts. Fuel 2004;83:1717–26.
[17] Da Costa P, Manoli JM, Potvin C, Djéga-Mariadassou G. Deep HDS on doped molybdenum carbides: From probe molecules to real feedstocks. Catal Today 2005;107–108:520–30.
[18] Sousa LA, Zotin JL, Da Silva VT. Hydrotreatment of sunflower oil using supported molybdenum carbide. Appl Catal A: Gen 2012;449:105–11.
[19] Wang H, Yan S, Salley SO, Simon Ng KY. Support effects on hydrotreating of soybean oil over NiMo carbide catalyst. Fuel 2013;111:81–7.
[20] Afanasiev P. New single source route to the molybdenum nitride Mo_2N. Inorgan Chem 2002;41(21):5317–9.
[21] Prasada Rao TSR, Murali Dhar G. Recent Advances in Basic and Applied Aspects of Industrial Catalysis. Dehradum, India: Elsevier; 1998.
[22] Schuit GCA, Gates BC. Chemistry and engineering of catalytic hydrodesulfurization. AIChE J 1973;3(19):417–38.
[23] Dimitriadis A, Bezergianni S. Co-hydroprocessing gas-oil with residual lipids: effect of residence time and H_2/Oil ratio. J Clean Prod 2016;131:321–6.
[24] Walendziewski J, Stolarski M, Łużny R, Klimek B. Hydroprocessing of light gas oil – rape oil mixtures. Fuel Process Technol 2009;90:686–91.
[25] Mochida I, Choi KH. An overview of hydrodesulfurization and hydrodenitrogenation. J Jpn Pet Inst 2004;47(3):145–63.
[26] Fooladi A, Samie M, Dashti A, Shandiz M. Simulation of a non-isothermal industrial hydrotreating reactor using simulink. Energy Fuels 2014;28:4828–34.
[27] Bezergianni S, Dimitriadis A. Temperature effect on co-hydroprocessing of heavy gas oil-waste cooking oil mixtures for hybrid diesel production. Fuel 2013;103:579–84.
[28] Dhandapani B, Clair TST, Oyama ST. Simultaneous hydrodesulfurization, hydrodeoxygenation, and hydrogenation with molybdenum carbide. Appl Catal A: Gen 1998;168:219–28.
[29] Qin Y, Chen P, Duan J, Han J, Lou H, Zheng X, et al. Carbon nanofibers supported molybdenum carbide catalysts for hydrodeoxygenation of vegetable oils. RSC Adv 2013;3:17485–91.
[30] Wang ZM, Han X, Zhang J, Wang ZL. In situ observation of CO_2 corrosion under high pressure. Corros Eng Sci Technol 2014;49(5):352–6.
[31] Bezergianni S, Dagonikou V. Effect of CO2 on catalytic hydrotreatment of gas oil. Can J Chem Eng 2015;93:1017–23.
[32] Sundaramurthy V, Dalai AK, Adjaye J. Comparison of P-containing γ-Al_2O_3 supported Ni-Mo bimetallic carbide, nitride ad sulfide catalysts for HDN and HDS of gas oils derived from Athabasca bitumen. Appl Catal A: Gen 2006;311:155–63.